

# Simulation Study of Thin-Body Ballistic n-MOSFETs Involving Transport in Mixed $\Gamma$ -L Valleys

Saumitra R. Mehrotra, Michael Povolotskiy, Doron Cohen Elias, Tillmann Kubis, Jeremy J. M. Law, Mark J. W. Rodwell, and Gerhard Klimeck

**Abstract**—Transistor designs based on using mixed  $\Gamma$ -L valleys for electron transport are proposed to overcome the density of states bottleneck while maintaining high injection velocities. Using a self-consistent top-of-the-barrier transport model, improved current density over Si is demonstrated in GaAs/AlAsSb, GaSb/AlAsSb, and Ge-on-insulator-based single-gate thin-body n-channel metal–oxide–semiconductor field-effect transistors. All the proposed designs successively begin to outperform strained-Si-on-insulator and InAs-on-insulator (InAs-OI) in terms of ON-state currents as the effective oxide thickness is reduced below 0.7 nm. InAs-OI still exhibits the lowest intrinsic delay ( $\tau$ ) due to its single  $\Gamma$  valley.

**Index Terms**—GaAs, GaSb, Ge, InAs, L-valley, Si, tight-binding (TB), ultrathin body (UTB).

## I. INTRODUCTION

HIGH-MOBILITY III–V’s are projected to be a material of choice for post-Si complementary metal–oxide–semiconductor logic [1]. These III–V materials exhibit high bulk electron mobility because of the light  $\Gamma$  valley that forms its conduction band edge ( $E_C$ ). A light effective mass also leads to low density of states (DOS), and consequently III–V channel materials provide diminishing benefit over Si as the effective oxide thickness (EOT) is scaled below 0.6 nm [2]. This loss of DOS can be compensated, under (111) confinement, using several eigenstates of the highly anisotropic L[111] band-edge states, or by aligning the  $\Gamma$  and lowest-energy L[111] band-edge states (Table I) [3], [5]. Previous works contributing toward this idea assumed an idealized interface at the bottom surface of the channel [5]. Another work considered channel thickness ( $t_{ch}$ ) large enough that

Manuscript received June 6, 2013; revised June 30, 2013; accepted July 9, 2013. Date of publication July 22, 2013; date of current version August 21, 2013. This work was supported in part by the National Science Foundation (NSF) under Grant EEC-0228390 that funds the Network for Computational Nanotechnology, the NSF National Robotics Initiative under Grant ECCS-1125017, Semiconductor Research Corporations under Grant SRC Task 2141, and Grant SRC Task 2273. The review of this letter was arranged by Editor M. Passlack.

S. R. Mehrotra, M. Povolotskiy, T. Kubis, and G. Klimeck are with the Network for Computational Nanotechnology and Birck Nanotechnology Center, Purdue University, West Lafayette, IN 47907 USA (e-mail: saumitra.r@gmail.com).

D. C. Elias, J. J. M. Law, and M. J. W. Rodwell are with the School of Electrical and Computer Engineering, University of California, Santa Barbara, CA 93106-9560 USA.

Color versions of one or more of the figures in this letter are available online at <http://ieeexplore.ieee.org>.

Digital Object Identifier 10.1109/LED.2013.2273072

TABLE I

BULK  $\Gamma$ - AND L-VALLEY BAND-EDGES AND BAND-EDGE MASSES [7]. BARRIER HEIGHT ( $E_b$ ) DIFFERENCE AND VALLEY TYPE ARE ALSO SHOWN (\* USING  $sp^3d^5s^*$  TB MODEL [8])

(111) designs	$E_L-E_\Gamma$	$E_b-E_\Gamma$	$m^*/m_0(L)$	$m^*/m_0(\Gamma)$	Type
GaAs*/AlAsSb/InP	385meV	620meV	$m_t = 0.09$ $m_l = 1.73$	$m = 0.046$	$\Gamma$ -L
GaSb/AlAsSb/GaSb	63meV	458meV	$m_t = 0.10$ $m_l = 1.3$	$m = 0.04$	L
Ge-OI	-	-	$m_t = 0.08$ $m_l = 1.58$	-	L

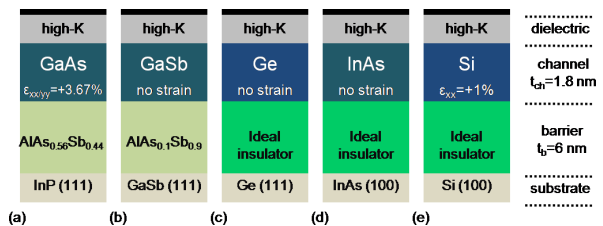


Fig. 1. SG-ETB MOSFET designs (channel/barrier/substrate) involving  $\Gamma$ -L valleys (a) GaAs/AlAs<sub>0.56</sub>Sb<sub>0.44</sub>/InP, (b) GaSb/AlAs<sub>0.1</sub>Sb<sub>0.9</sub>/GaSb, and (c) Ge-OI along with (d) InAs-OI and (e) tensile strained Si-OI.

renders it unsuitable for a well-behaved single-gate (SG)-metal–oxide–semiconductor field-effect transistor (MOSFET) at sub-10-nm channel length [4]. To maintain gate control as channel ( $L_g$ ) is scaled to sub-10-nm lengths,  $t_{ch} < 3$  nm is needed in SG-MOSFETs [6]. In this letter, SG extremely-thin-body (ETB)-MOSFET designs on (111) [Fig. 1(a)–(c)] are studied and the results are compared against InAs-on-insulator (InAs-OI) [Fig. 1(d)] and 1% tensile strained Si-on-insulator (Si-OI) [Fig. 1(e)] in the ballistic regime at a channel thickness of  $t_{ch} = 1.8$  nm.

## II. DEVICE STRUCTURE

Realistic approaches toward designing a (111) SG-ETB-MOSFET requires a careful choice of the channel material, along with a suitable barrier material to confine the carriers, and a suitable substrate for fabrication (Fig. 1). The idea behind (111) SG-ETB-MOSFETs is to quantize the anisotropic bulk L-valley, leading to the formation of multiple L[111] subbands with light in-plane transport mass [3]. This necessitates either a channel material which in bulk has its L-valley either below (e.g., Ge) or only slightly above that of the  $\Gamma$  valley (e.g., GaSb), such that in the thin, quantized channel the

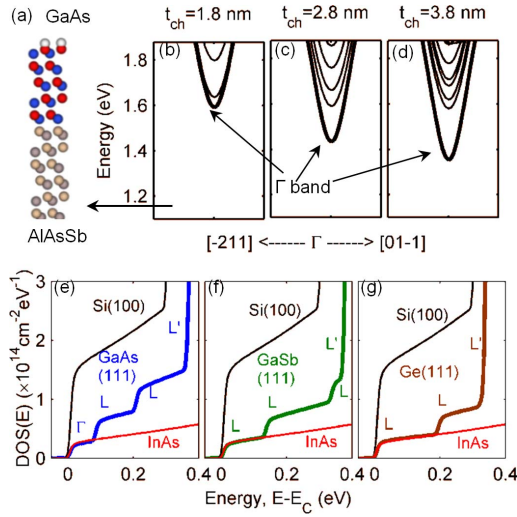


Fig. 2. (a) Atomistic representation of the GaAs/AlAsSb/InP (111) device structure [Fig. 1(a)]. Calculated band structure of GaAs/AlAsSb/InP (111) with GaAs thickness ( $t_{ch}$ ) as (b) 1.8 nm, (c) 2.8 nm, and (d) 3.8 nm. The  $\Gamma$  subband is highlighted in bold. Calculated DOS(E) versus energy for the (e) GaAs/AlAsSb (111), (f) GaSb/AlAsSb (111), and (g) Ge-OI along with Si-OI (100) and InAs-OI (100) for comparison.

L[111] eigenstates are the lowest in energy. A low transport mass with increased DOS can also be obtained by aligning in energy the quantized  $\Gamma$  and L[111] subbands in materials having a moderate (0.1–0.4 eV)  $\Gamma$ -L separation in the bulk (e.g., GaAs).

Although we have considered and analyzed many channel designs, we here report in detail only those cases showing high performance [9]. Tensile-strained GaAs/AlAs<sub>0.56</sub>Sb<sub>0.44</sub>/InP (111) [Fig. 1(a)] was chosen as it is the only case providing  $\Gamma$ -L alignment among any composition of strained In<sub>x</sub>Ga<sub>1-x</sub>As/AlAs<sub>0.56</sub>Sb<sub>0.44</sub>/InP (111) for the device structure considered here [10]. Another possible candidate, lattice-matched GaAs<sub>0.5</sub>Sb<sub>0.5</sub>/AlAs<sub>0.56</sub>Sb<sub>0.44</sub>/InP (111) is not discussed here as the confinement of the L-valley bound state is poor, making  $\Gamma$ -L alignment difficult. The strained In<sub>x</sub>Ga<sub>1-x</sub>Sb cases were not considered because of the lack of available tight-binding (TB) parameters at the time of the study. In addition, the barrier material, for the channel designs in Fig. 1(c)–(e), is assumed to be an ideal insulator with  $k = 3.9$  because of the lack of available oxide TB parameters. For all the cases considered, a channel body thickness of  $t_{ch} = 1.8$  nm and a barrier thickness,  $t_b = 6$  nm were used (Fig. 1). Note that at  $t_{ch} = 1.8$  nm, the  $\Gamma$ -L valley separation is  $< 100$  meV for the GaAs/AlAs<sub>0.56</sub>Sb<sub>0.44</sub>/InP(111) design [Fig. 2(b)]. The III–V (111)  $\Gamma$ -L channel designs are compared with L-valley transport in (111) Ge-on-insulator (Ge-OI) [Fig. 1(c)],  $\Gamma$ -valley transport in InAs-OI [Fig. 1(d)] and to uniaxial tensile strained (100) Si-OI [Fig. 1(e)] on (100). As in [4]–[6], for all cases [Fig. 1(a)–(e)], wavefunction penetration into the gate dielectric is neglected, because of the lack of available oxide TB parameters. Because of the strong sensitivity of  $\Gamma$ -L energy alignment to the bottom barrier boundary conditions, transport modeling for the (111) GaAs [Fig. 1(a)] and GaSb [Fig. 1(b)] designs explicitly includes both the parameters of both the channel and the bottom barrier.

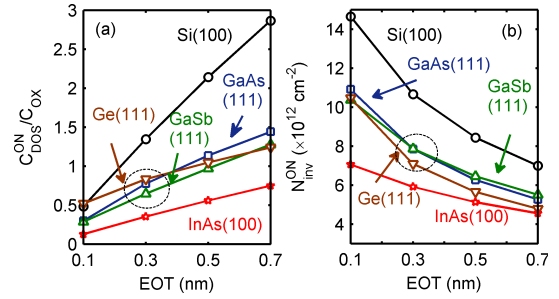


Fig. 3. Calculated ON-state (a)  $C_{DOS}^{ON}/C_{OX}$  and (b) inversion charge,  $N_{inv}^{ON}$  as a function of EOT.  $\Gamma$ -L minima designs are identified by a circle.

### III. SIMULATION APPROACH

$I_{DS}$ - $V_{GS}$  characteristics are simulated using a semiclassical top-of-the-barrier transport model by solving the 3-D atomistic Schrödinger (based on  $sp^3d^5s^*$  TB model) and 1-D Poisson equation in a self-consistent fashion [11], [12]. The TB parameters are adjusted to conform to the bandgaps and  $\Gamma$ -L separations recommended by Vurgaftman [7]. The barrier materials are included in the Schrödinger domain for GaAs [Fig. 1(a)] and GaSb [Fig. 1(b)]. Because the wavefunctions extend into the barriers, the energy minima and E-k dispersion of the bound states depend significantly upon the properties of the barrier materials, and we find here different valley energy alignments than if these barriers are neglected [10]. The barriers are sufficiently thick for the wavefunctions of the populated bound states to decay to negligible values at the barriers' bottom surfaces; making the simulations insensitive to the substrate parameters. The substrate material is therefore not included in simulations. Lattice mismatch, hence material strain, is of course included in the simulations, i.e., 3.67% in-plane tensile biaxial strain in GaAs [Fig. 1(a)] and 1% uniaxial tensile strain in Si [Fig. 1(e)] [8]. For the cases in Fig. 1(c)–(e), the bottom barrier was treated as an ideal insulator with zero wavefunction penetration. In all cases considered, the gate dielectric is treated as an ideal insulator with zero wavefunction penetration. A zero-electric field boundary condition is applied at the bottom of the barrier to mimic the continuity of the potential profile. The transport direction for all the cases is taken to be  $\langle 110 \rangle$  except InAs-OI, for which the transport direction is  $\langle 100 \rangle$ . It should be pointed that InAs has a  $\Gamma$ -L separation of 0.716 eV [7]–1.16 eV [8]. This will lead to only  $\Gamma$ -valley subbands forming similar band edge profiles in the relevant energy range with (100), (110), or (111) surface confinement. The ON-state is defined at  $V_{DS} = V_{GS} = 0.6$  V, with the threshold voltage set such that off-state current is  $I_{DS}^{OFF} = 0.1 \mu A/\mu m$  [4], [5]. To capture the effect of the increasing dielectric capacitance, the simulations were performed for EOT values ranging from 0.1 to 0.7 nm and subsequently ON-state characteristics were extracted.

### IV. RESULTS

The nearly 4:1 difference in DOS between Si and InAs can be readily noted in Fig. 2(e)–(g). The low DOS is improved by populating two L[111]-valley subbands for GaSb

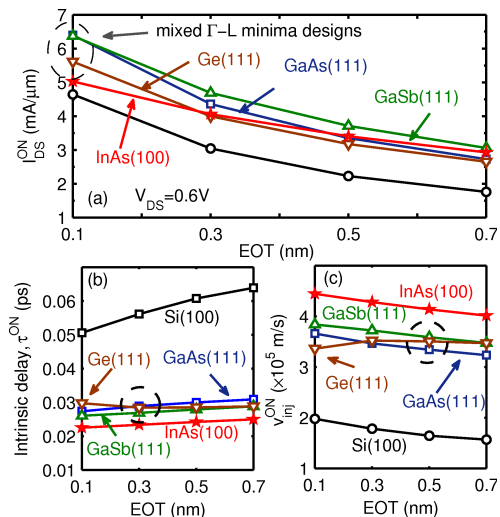


Fig. 4. Calculated ON-state (a) drain current, (b) intrinsic transit delay,  $\tau_{ON}^{ON}$  (assuming  $L_g = 10$  nm), and (c) injection velocity,  $v_{inj}^{ON}$  for the different ETB-MOSFET cases as a function of EOT.

[Fig. 2(f)] and Ge [Fig. 2(g)], while the  $\Gamma$  and first two subbands of L[111] are populated for GaAs(111). On moving deeper inside the energy range, the DOS shows a huge jump due to contributions from the non-L[111]-valleys labeled as  $L'$  [Fig. 2(e)–(g)]. We will refer to the (111) GaSb, Ge, and GaAs cases [Fig. 1(a)–(c)] as mixed  $\Gamma$ -L minima designs. The DOS bottleneck occurs when the DOS capacitance ( $C_{DOS} = q^2 dN_{inv}/dE_{fs}$ ) begins to dominate over the dielectric capacitance,  $C_{OX}$  i.e.,  $(C_{DOS}/C_{OX}) < 1$ , nullifying the expected gains as EOT is scaled to smaller values. From Fig. 3(a), it can be seen that InAs (100) suffers from DOS bottleneck at all the values of EOT  $< 0.7$  nm. It should also be noticed that as the EOT is scaled, first  $\Gamma$ -L minima designs at EOT  $\simeq 0.4$  nm and Si (100) at EOT  $\simeq 0.2$  nm also begin to be  $C_{DOS}$  limited. Therefore, as shown in Fig. 3(b), Si (100) exhibits the highest ON-state carrier density while InAs (100) has the lowest ON-state carrier density. It should also be noted that as the EOT is scaled from 0.7 to 0.1 nm, InAs-OI shows  $\sim 1.5X$  increment in ON-state inversion carrier density, while both Si (100) and mixed  $\Gamma$ -L minima designs exhibit  $\sim 2X$  increment in ON-state inversion carrier density. This highlights the relative advantage of higher DOS as dielectrics are thinned.

Fig. 4(a) shows the ON-state currents for the different ETB MOSFET cases. Note that even for 0.1-nm EOT, InAs (100) shows larger  $I_{DS}^{ON}$  than Si (100). This conclusion differs from that of [2] because of the thin 1.8-nm channel considered here. Given the strongly nonparabolic InAs  $\Gamma$  valley, the  $E_C$  edge mass increases from its bulk value of 0.023 to 0.08  $m_0$  for a 1.8-nm thin quantum well [3], [8]. Simultaneously, the proposed  $\Gamma$ -L minima designs begin to outperform InAs (100) as EOT is scaled. In terms of the ON-state current, GaSb outperforms InAs at EOT = 0.7 nm, GaAs outperforms InAs at EOT = 0.5 nm, and Ge outperforms InAs at EOT = 0.3 nm. At the extreme limit of EOT = 0.1 nm, GaAs and GaSb deliver  $\sim 27\%$  more current than InAs and  $\sim 36\%$  more current than Si. As a consequence of top-of-the-barrier transport model,

all the designs exhibit an ideal subthreshold slope (SS) of 60 mV/decade [11]. The impact of short-channel effects can further degrade the SS. Further reduction in the ballistic ON-state current can be expected due to carrier scattering and parasitic resistances [6]. The calculated transit delay  $\tau_{ON}^{ON} (= L_g/v_{inj}^{ON})$  at the ON-state is shown in Fig. 4(b). InAs exhibits the lowest delay because of higher injection velocity ( $v_{inj}$ ), as shown in Fig. 4(c). Note that gate delay is a function not only of FET gate-channel capacitance ( $= \tau_{ON}^{ON} I_{ON}/V_{DD}$ ), but also of interconnect capacitance and of gate-source and gate-drain fringing capacitances.

## V. CONCLUSION

In this letter, SG-ETB designs that include GaAs/AlAsSb/InP (111), GaSb/AlAsSb/GaSb (111), and Ge-OI (111), that provide both high charge density and high carrier velocity in highly scaled MOSFETs are presented. The performance of the proposed  $\Gamma$ -L minima designs has been compared against InAs-OI (100) and tensile strained Si-OI (100) MOSFETs at the same channel body thickness of 1.8 nm in the ballistic limit. All designs provide larger ON-current than InAs-OI (100) for EOT  $< 0.3$  nm. The proposed transistor designs allow a scope for MOSFET performance improvements even at the extreme EOT scaling limits. Future work would include quantum transport simulations including carrier scattering and source-drain tunneling, that becomes more relevant as  $L_g$  is scaled to sub-10 nm.

## REFERENCES

- [1] J. A. del Alamo, "Nanometre-scale electronics with III-V compound semiconductors," *Nature*, vol. 479, no. 7373, pp. 317–323, Nov. 2011.
- [2] M. Fischetti, L. Wang, B. Yu, *et al.*, "Simulation of electron transport in high-mobility MOSFETs: Density of states bottleneck and source starvation," in *Proc. IEEE IEDM*, Dec. 2007, pp. 109–112.
- [3] M. Rodwell, W. Frensky, S. Steiger, *et al.*, "III-V FET channel designs for high current densities and thin inversion layers," in *Proc. DRC*, Jun. 2010, pp. 149–152.
- [4] M. Luisier, "Performance comparison of GaSb, strained-Si, and InGaAs double-gate ultrathin-body n-FETs," *IEEE Electron Device Lett.*, vol. 32, no. 12, pp. 1686–1688, Dec. 2011.
- [5] R. Kim, T. Rakshit, R. Kotlyar, *et al.*, "Effects of surface orientation on the performance of idealized III-V thin-body ballistic n-MOSFETs," *IEEE Electron Device Lett.*, vol. 32, no. 6, pp. 746–748, Jun. 2011.
- [6] S. H. Park, Y. Liu, N. Kharche, *et al.*, "Performance comparisons of III-V and strained-Si in planar FETs and nonplanar FinFETs at ultrashort gate length (12 nm)," *IEEE Trans. Electron Devices*, vol. 59, no. 8, pp. 2107–2114, Aug. 2012.
- [7] I. Vurgaftman, J. R. Meyer, and L. R. Ram-Mohan, "Band parameters for III-V compound semiconductors and their alloys," *J. Appl. Phys.*, vol. 89, no. 11, pp. 5815–5875, 2001.
- [8] T. B. Boykin, G. Klimeck, R. C. Bowen, *et al.*, "Diagonal parameter shifts due to nearest-neighbor displacements in empirical tight-binding theory," *Phys. Rev. B*, vol. 66, pp. 125207-1–125207-6, Sep. 2002.
- [9] S. Mehrotra, "Nanoscale transistors: Performance at the scaling limits," Ph.D. dissertation, School Electr. Comput. Eng., Purdue Univ., West Lafayette, IN, USA, 2013.
- [10] S. Mehrotra, M. Povolotskyi, J. Law, *et al.*, "Design of high-current L-valley GaAs/AlAsSb/InP (111) ultra-thin-body nMOSFETs," in *Proc. Int. Conf. IPRM*, Aug. 2012, pp. 151–154.
- [11] A. Paul, S. Mehrotra, G. Klimeck, *et al.*, "On the validity of the top of the barrier quantum transport model for ballistic nanowire MOSFETs," in *Proc. 13th Int. Workshop Comput.*, May 2009, pp. 1–4.
- [12] S. Steiger, M. Povolotskyi, H.-H. Park, *et al.*, "NEMO5: A parallel multiscale nanoelectronics modeling tool," *IEEE Trans. Nanotechnol.*, vol. 10, no. 6, pp. 1464–1474, Nov. 2011.